HHS Public Access

Author manuscript

J Endocrinol. Author manuscript; available in PMC 2021 January 01.

GLIS3 binds pancreatic beta cell regulatory regions alongside other islet transcription factors

David W. Scoville, **Kristin Lichti-Kaiser**, **Sara A. Grimm**, **Anton M. Jetten**

Cell Biology Group, Immunity, Inflammation and Disease Laboratory, National Institute of Environmental Health Sciences, National Institutes of Health, Research Triangle Park, NC 27709, USA

Abstract

The Krüppel-like zinc finger transcription factor Gli-similar 3 (GLIS3) plays a critical role in the regulation of pancreatic beta cells, with global *Glis3* knockout mice suffering from severe hyperglycemia and dying by post-natal day 11. In addition, GLIS3 has been shown to directly regulate the early endocrine marker *Ngn3*, as well as *Ins2* gene expression in mature beta cells. We hypothesize that GLIS3 regulates several other genes critical to beta cell function, in addition to *Ins2*, by directly binding to regulatory regions. We therefore generated a pancreas-specific *Glis3* deletion mouse model (*Glis3*$^{\Delta pan c}$) using a *Pdx1*-driven Cre mouse line. Roughly 20% of these mice develop hyperglycemia by 8-weeks and lose most of their insulin expression. However, this did not appear to be due to loss of the beta cells themselves, as no change in cell death was observed. Indeed, presumptive beta cells appeared to persist as PDX1^{+}/INS^{-}/MAFA^{-}/GLUT2^{-} cells. Islet RNA-seq analysis combined with GLIS3 ChIP-seq analysis revealed apparent direct regulation of a variety of diabetes related genes, including *Slc2a2* and *Mafa*. GLIS3 binding near these genes coincided with binding for other islet-enriched transcription factors, indicating these are distinct regulatory hubs. Our data indicates that GLIS3 not only regulates insulin expression, but several additional genes critical for beta cell function.

Keywords

GLIS3; beta cells; RNA-seq; ChIP-seq; transcription factor; gene regulation

Introduction

GLIS3 belongs to the GLIS subfamily of Krüppel-like proteins that are most closely-related to members of the GLI and ZIC families (Jetten, 2018). It plays a critical role in the regulation of various physiological processes, including pancreas development, osteogenesis, kidney function and thyroid hormone regulation and is implicated in several major human pathologies (e.g., diabetes, hypothyroidism, cancer, cystic kidney disease) (Dimitri et al., 2011, Wen and Yang, 2017, Scoville et al., 2017, Jetten, 2018). GLIS3

Corresponding author: Anton M. Jetten, National Institute of Environmental Health Sciences, National Institutes of Health, 111 TW Alexander Drive, Research Triangle Park, NC, USA 27709, jetten@niehs.nih.gov.

Declaration of Interest: We have no conflict of interest that could be perceived as prejudicing the impartiality of the research reported

contains five Krüppel-like zinc finger motifs that recognize specific DNA sequences in regulatory regions of target genes allowing it to function as a transcriptional activator and/or repressor (Kang et al., 2010, Lichti-Kaiser et al., 2012). Genetic aberrations in human *GLIS3* are associated with a rare syndrome characterized by Neonatal Diabetes and congenital Hypothyroidism (NDH). Depending on the nature of the mutation, additional features have included hepatic fibrosis, congenital glaucoma, polycystic kidney disease, facial dysmorphism, and osteopenia (Senee et al., 2006, Dimitri et al., 2011, Habeb et al., 2012). Additional evidence for a role of GLIS3 in diabetes comes from genome-wide association studies (GWAS) that link *GLIS3* variants to aberrant glucose regulation and reduced beta cell function, and identified *GLIS3* as a risk locus for both type-1 and type-2 diabetes (Barrett et al., 2009, Dupuis et al., 2010, Cho et al., 2011, Liu et al., 2011, Rees et al., 2011).

GLIS3 protein expression in the mouse pancreas is first observed at embryonic day 13.5 in bipotent pancreatic progenitor cells (i.e. cells of capable of differentiating into ductal or endocrine cells (Zhou et al., 2007)), and its expression is maintained in both lineages into adulthood (Kang et al., 2016). Within the mature endocrine population, GLIS3 is restricted to beta cells and pancreatic polypeptide cells (Kang et al., 2016). We and others have previously demonstrated that global *Glis3*-null mice die by post-natal day 11 (PND11) due to neonatal diabetes (Kang et al., 2009, Watanabe et al., 2009, Yang et al., 2009). Islet size and the expression of several beta cell markers, including *Ins2*, the glucose transporter *Slc2a2*, *MafA*, and *Nkx6.1* were dramatically decreased in *Glis3*-null mice. Indeed, GLIS3 is critical for *Ins2* expression in mature beta cells through its interaction with other known regulators of *Ins2*, such as PDX1, NEUROD1, and MAFA (Kang et al., 2009, ZeRuth et al., 2013, Yang et al., 2009). However, the precise role of GLIS3 in the maintenance of functional beta cells, aside from regulating insulin expression, remains poorly defined.

To gain greater insights into the regulatory functions of GLIS3 in the pancreas, we generated a pancreas-specific *Glis3* knockout mouse model. $Glis3^{fl/fl}$ mice were crossed with mice expressing Cre-recombinase under the control of the *Pdx1* gene promoter to generate a pancreas-specific knockout model ($Glis3^{\Delta panc}$). We were thus able to separate the pancreatic phenotype from other organs affected by global *Glis3* loss, such as the kidney and thyroid. The major objective of this study was to obtain a better understanding of GLIS3-mediated regulation of gene transcription in pancreatic islets, we therefore performed gene expression analysis on islets from these mice, as well as GLIS3 ChIP-seq analysis. In addition, we compared these results to publicly available data on the genomic binding of several other islet-enriched transcription factors, in order to determine whether GLIS3 regulates pancreatic beta cell gene transcription by binding to distinct regulatory hubs with other islet transcription factors (Hu and Tee, 2017). Our study shows that GLIS3 plays a critical role in directly regulating a number of genes associated with beta cell identity, maturation, and function, and suggests that GLIS3 performs these regulatory functions in association with other islet-enriched transcription factors.

Materials and Methods

Generation of pancreas-specific Glis3 knockout mice.

A conditional knockout allele for the *Glis3* gene was generated in C57BL/6J mice using homologous recombination in mouse embryonic stem cells and subsequent blastocyst injection of the appropriate targeted ES cells (C57BL/6-Glis3<tm2Amj>). The vector contained loxP sites flanking exon 5 of *Glis3*, which included part of the DNA binding domain (Figure1A). Previous work has shown that deletion of any part of the DNA binding domain produces a non-functional protein (Beak et al., 2008). Mice were bred with a strain expressing Cre recombinase under the control of the *Pdx1* promoter, which produces pancreas-specific deletion by e10.5 (Jackson Laboratories Stock No. 014647) (Hingorani et al., 2003). Animal studies followed guidelines outlined by the NIH Guide for the Care and Use of Laboratory Animals and protocols were approved by the Institutional Animal Care and Use Committee at the NIEHS.

Blood Glucose measurements.

Tail blood was collected from wild type ($Glis3^{fl/fl}$) and $Glis3^{\Delta panc}$ mice at indicated time points. Glucose levels were measured with Nova Max glucose monitoring system (Nova Biomedical; Waltham, MA).

Immunohistochemical analysis.

Mouse pancreases were fixed for 4 hours in 4% paraformaldehyde in PBS and embedded in OCT (Tissue Tek; Hatfield, PA) prior to cryogenic sectioning. Primary antibodies are listed in Supplementary Table 1. DBA-Fluorescein was purchased from Vector Labs (Burlingame, CA). Alexa Fluor-conjugated secondary antibodies were purchased from Molecular Probes (Carlsbad, CA). Nuclei were stained with DAPI Prolong Diamond from Invitrogen (Carlsbad, CA). Fluorescent images were captured using a Zeiss LSM 880 confocal microscope and ZEN software.

Proliferation and TUNEL Staining.

2-week old pancreases were stained with antibodies against PDX1 and either Ki67 or the DeadEnd™ Fluorometric TUNEL System (Promega #G3250) following manufacturer's protocol. At least 6 sections >200 microns apart per mouse from 3 mice per genotype were examined using confocal microscopy (Zeiss LSM 880 with Airyscan), and co-localization quantified manually using ImageJ (NIH, Bethesda, MD).

Islet isolation and qRT-PCR analysis.

Pancreatic islets were isolated via collagenase injection through the common bile duct into the pancreas, followed by digestion and hand-picking. RNA was isolated using Trizol reagent (Life Technologies) followed by DNAse I digestion and additional purification via Ambion RNAqueous micro kit (Ambion). cDNA was synthesized using a High Capacity DNA Reverse Transcription Kit (Applied Biosystems; Foster City, CA). qRT-PCR was carried out in triplicate in a StepOnePlus Real Time PCR System (Applied Biosystems;

Foster City, CA). All results were normalized to *Gapdh* expression and are shown relative to control using the $2^{\Delta\Delta ct}$ method. Primer sequences are listed in Supplementary Table 1.

RNA sequencing.

Islets were isolated from 4-week old *Glis3*$^{\Delta panc}$ and control littermates (*Glis3*$^{fl/fl}$). ~10 ng of RNA was converted to cDNA using the high capacity cDNA reverse transcription kit (Applied Biosystems), and islet RNA from mice with a 78–91% removal of Glis3 (as measured by qRT-PCR of the deleted exon) were submitted for RNA-seq analysis at the NIEHS Epigenomics Core (with control littermates). Briefly, RNA was converted to cDNA using the NextFlex Rapid RNA seq kit (Illumina), and sequenced as paired-end 76mers on a NextSeq500 (Ilumina) for each sample (N=4 *Glis3*$^{fl/fl}$, 3 *Glis3*$^{\Delta panc}$). Read pairs were filtered to retain only those with a mean base quality score of at least 20 for each end. Adapter was clipped from the end of each read via Cutadapt v1.2.1 (Martin, 2011) (parameters: -a AGATCGGAAGAG -O 5 -q 0), then read pairs were filtered to retain only those at least 30nt in length after adapter removal. Trimmed and filtered read pairs were aligned against the mm10 reference assembly via STAR v2.5 (Dobin et al., 2013) (parameters: --alignSJoverhangMin 8 --limitBAMsortRAM 55000000000 --outSAMstrandField intronMotif --outFilterIntronMotifs RemoveNoncanonical). Counts per gene were determined by Subread featureCounts v1.5.0-p1 (Liao et al., 2014) (parameters: -s0 -Sfr -p) for a set of gene models defined by RefSeq transcripts as downloaded from the UCSC Table Browser (http://genome.ucsc.edu/cgi-bin/hgTables) as of November 7, 2017. Differentially expressed genes were identified via DESeq2 v1.10.1 (Love et al., 2014) at an FDR threshold of 0.05, and a complete list is provided in Supplementary Table 2. For RNA-seq genome browser views, replicates were merged and normalized to 50 million mappable reads.

ChIP sequencing.

Islets from 8-week old GLIS3-EGFP mice (Kang et al., 2016) were isolated, flash frozen at −80°C. ChIP-seq analysis was performed by Active Motif (Carlsbad, CA). ChIP was performed using a GFP antibody and ~1,800 islets. Input and ChIP samples were run as single-end 75mers on a NextSeq500 (Illumina); 42–43 million reads each were obtained for each. Raw data is available from Gene Expression omnibus (GSE122120). For comparison to other published ChIP-seq data, raw sequencing data was obtained from GEO for: NKX2.2 (GSE79785), MAFA and NEUROD1 (GSE30298), PDX1 and FOXA2 (SRA008281), NKX6.1 (GSE40975), ISL1 and LDB1 (GSE84759) and from ArrayExpress for: PDX1 (E-MTAB-1143). For consistency, all ChIP-seq datasets were processed by the same workflow, as follows. Reads were filtered to retain only those with a mean base quality score of at least 20. Adapter was clipped from the end of each read via Cutadapt v1.2.1 (Martin, 2011) (parameters: -a AGATCGGAAGAG -O 5 -q 0), then reads were filtered to retain only those at least 30nt in length after adapter removal. Trimmed and filtered reads were aligned against the mm10 reference assembly via Bowtie v1.2 (Langmead et al., 2009), retaining only uniquely-mapped reads (parameter: -m 1). For samples with multiple sequencing runs, replicates were combined with MergeSamFiles.jar from the Picard tool suite v1.110. Duplicate reads were removed with MarkDuplicates.jar from the Picard tool suite v1.110. For visualization of mapped read depth on the UCSC Genome Browser, uniquely-mapped

non-duplicate reads were extended to 200nt, converted to bedGraph format using BEDTools v2.24.0 genomeCoverageBed (Quinlan and Hall, 2010), then normalized to 10 million reads per sample. Peak calling was performed with HOMER v4.9.1 (Heinz et al., 2010), with parameters: -style factor -fdr 0.00001. The matched input sample was used as background if available. For public samples with no available matched input, a surrogate input of 20 million reads was generated by aggregating randomly-selected (uniquely-mapped non-duplicate) reads from the mouse islet input samples from GSE40975, GSE84759, E-MTAB-1143, and our current dataset. Called peaks from each dataset were re-defined as 200mers centered on the midpoint of the original peak call. A complete list of nearest genes bound by GLIS3 is included in Supplementary Table 3.

Pathway Analysis.

Pathway analysis was performed via DAVID tools (v6.8) for KEGG pathway analysis (Huang da et al., 2009b, Huang da et al., 2009a). Full list of pathways and genes are included in Supplementary Tables 4–6. Pathview analysis was performed using the online tool, as described (Luo et al., 2017).

Luciferase reporter assay.

HEK293T cells were grown in DMEM containing 10% Fetal Bovine Serum (FBS) and penicillin/streptomycin. Cells were transfected using Lipofectamine 2000 (Invitrogen) with 100 ng of luciferase reporter plasmid (pGL4.27) under the control of the MafA Region 3 regulatory sequence (Raum et al., 2006)), 50 ng of CMV-driven beta-galactosidase plasmid, and 100 ng of either CMV-driven mouse Glis3 or a control plasmid. Twenty-four hours after transfection, cells were lysed with Passive Lysis Buffer (Promega), and luciferase activity was measured with a Luciferase Assay System (Promega) and beta-galactosidase measured with a Luminescent Beta-Galactosidase Detection kit II (Takara) according to the manufacturer's protocols. Transfections were performed in triplicate, with each experiment performed at least 3 times.

Statistical Analysis.

Where indicated, statistics were calculated using a two-tailed student t-test. Significance indicates a p-value <0.05, unless otherwise specified.

Results

Glis3$^{\Delta panc}$ mice develop hyperglycemia due to loss of insulin expression.

In order to investigate the role of GLIS3 in the pancreas, we generated a pancreas-specific *Glis3* deletion mouse model. *Glis3*$^{fl/fl}$ mice containing LoxP sites flanking exon 5 (Figure 1A), which encodes a portion of the DNA binding domain, were generated and crossed with a mouse strain expressing Cre-recombinase under regulation of the *Pdx1* promoter, expressed in the early stages of pancreatic development in the common pancreatic progenitor cells. *Glis3*$^{\Delta panc}$ mice did not develop neonatal diabetes like the global *Glis3* mutant mice, as their blood glucose levels were not significantly different at 2-weeks (data not shown). However, by 8-weeks of age, ~20% of *Glis3*$^{\Delta panc}$ mice developed severe hyperglycemia (>500 mg/dL blood glucose), while the remaining *Glis3*$^{\Delta panc}$ mice exhibited

glucose levels comparable to those of control littermates (Figure 1B). The development of hyperglycemia appears to relate to the efficiency of *Glis3* exon 5 removal, as mice with >75% deletion displayed mild hyperglycemia at 4-weeks (Supplementary Figure 1), consistent with *Pdx1-Cre* mosaic expression in pancreatic progenitor cells (Hingorani et al., 2003). Another investigator utilizing a similar Glis3 knockout strategy with a *Pdx1-Cre* model reported hyperglycemia in only a subset of *Glis3* knockout mice (Yang et al., 2017). In addition, partial Glis3 deletion in $Glis3^{\Delta panc}$ euglycemic mice appears to phenocopy Glis3 heterozygous mice, which are euglycemic, but are more susceptible to impaired glucose tolerance in high fat diet-induced obesity (Yang et al., 2013).

Immunofluorescent staining of pancreas sections from euglycemic and hyperglycemic $Glis3^{\Delta panc}$ mice and control littermates at 8-weeks of age (Figure 1C–F) revealed a loss of insulin expression in $PDX1^+$ presumptive beta cells, with a more severe loss of insulin observed in hyperglycemic animals (Figure 1C). We presume these cells are former beta cells due to their PDX1 expression and central location within the islet. Pancreatic polypeptide levels also appeared decreased (Figure 1D), consistent with our recent discovery of GLIS3 expression in pancreatic polypeptide cells (Kang et al., 2016). Glucagon and somatostatin expression appeared unaffected (Figure 1E–F), likely reflecting the lack of GLIS3 expression in the mature alpha and delta cells (Kang et al., 2016).

$Glis3^{\Delta panc}$ islet beta cells do not undergo apoptosis or dedifferentiation.

In order to further study these $PDX1^+$ presumptive beta cells, we stained for MAFA, a marker of mature beta cells in both mice and humans, and GLUT2, a beta cell specific glucose transporter. Expression of these markers was lost in most but not all $PDX1^+$ cells by 8-weeks of age (Figure 2A–B). Talchai et al. suggested that, under stress conditions, beta cells may dedifferentiate into an earlier point in endocrine lineage, as marked by NGN3 expression (Talchai et al., 2012). However, we did not detect re-expression of NGN3 at 8-weeks in the $PDX1^+$ cells (Supplementary Figure 2). Additionally, it is possible that the loss of insulin expression was due to decreased proliferation or increased apoptosis at an earlier timepoint. We therefore examined proliferation and apoptosis at 2-weeks of age, prior to the secondary effects of hyperglycemia seen at 8-weeks. $Ki67^+PDX1^+$ cells were slightly increased, indicating a slight increase in proliferation, whereas no increase in TUNEL staining was observed (Figure 2C–F). Correspondingly, we saw a slight, non-significant increase in the total number of Pdx1+ cells in $Glis3^{\Delta panc}$ mice (data not shown). This indicates that while islet $PDX1^+$ cells in $Glis3^{\Delta panc}$ mice no longer express insulin and are likely non-functional, these cells remain present within the islet in a dysfunctional state.

GLIS3 regulates many genes critical for beta cell identity and function.

In order to establish a global network of GLIS3-regulated genes, we performed RNA-seq analysis on isolated islets from $Glis3^{\Delta panc}$ mice at 4-weeks of age, prior to the onset of severe hyperglycemia (>500mg/dL) so as to limit its secondary effects. In total, 1,162 genes were found to be upregulated >1.5 fold, and 612 genes were found to be downregulated >1.5 fold upon loss of GLIS3, consistent with GLIS3's role as both an activator and repressor of gene expression (Supplementary Table 2). KEGG pathway analysis indicated that the downregulated genes were involved in a variety of pathways, including Maturity Onset

Diabetes of the Young (MODY) and insulin secretion, as well as a variety of metabolic pathways (Figure 3A). Examination of the insulin secretion pathway via Pathview analysis indicated that the expression of several insulin pathway-related genes was regulated by GLIS3, including downregulation of the GLP1 receptor (*Glp1r*) and IP3 receptor (*Itpr1*), along with *MafA* and *Slc2a2* (Figure 3B). The UCSC genome browser tracks in Figure 3C–D illustrate the significant downregulation of both *MafA* and *Slc2a2* mRNA expression, consistent with the immunofluorescent staining (Figure 2A–B). Downregulation of *Ins2* was also observed, consistent with the observations of other models of *Glis3* deletion (Supplementary Figure 3)(Watanabe et al., 2009, Kang et al., 2009, Yang et al., 2009, Yang et al., 2011, Yang et al., 2013, Nogueira et al., 2013, Yang et al., 2017, Amin et al., 2018).

GLIS3 binds to beta cell genes in mouse islets.

In order to establish which of these differentially expressed genes were directly regulated by GLIS3, we performed ChIP-seq analysis of GLIS3 in adult mouse islets. As no reliable GLIS3 antibody currently exists, we utilized a mouse model where the C-terminus of GLIS3 is fused to an enhanced GFP tag (GLIS3-GFP), thus allowing for precipitation with a GFP antibody. One of the top consensus binding sequences detected in our ChIP-seq analysis matched that of Zic/Gli/Glis family members, similar to the consensus of the GLIS3 binding site previously identified in the thyroid gland (Figure 4A and (Kang et al., 2017)), indicating the ChIP-seq was successful in detecting specific GLIS3 binding. A complete list of bound genes (i.e. nearest gene to GLIS3 binding peak) is provided in Supplementary Table 3. GLIS3 binding was most highly enriched at introns within the gene body and promoter regions, consistent with what was observed in GLIS3 ChIP-seq experiments in the thyroid (Figure 4B)(Kang et al., 2017). Similar to previous reports by our group (ZeRuth et al., 2013), GLIS3 binding was observed at the *Ins2* promoter (Figure 4C), as well as an enhancer for *Slc2a2* (Figure 4D). Interestingly, all of the genes examined with a known role in beta cell function display GLIS3 binding within 2kb of their transcriptional start site (Table 1). However, only some of these genes were downregulated in $Glis3^{\Delta panc}$ mice (Table 1), indicating that GLIS3 may not be essential for regulation of a fraction of these genes, or that their regulation by GLIS3 may be dependent upon upstream signaling events absent under the tested conditions. We also combined our ChIP-seq and gene expression data to examine more closely those genes directly regulated by GLIS3 (i.e. GLIS3-bound genes that are differentially expressed in $Glis3^{\Delta panc}$ mice). KEGG pathway analysis of these genes identified many of the same pathways as found by analyzing gene expression data alone (Figure 3A, Supplementary Figure 4). This highlights the important role GLIS3 binding plays in regulating proper beta cell function, as indicated by the hyperglycemic phenotype of the $Glis3^{\Delta panc}$ mice.

GLIS3 binding overlaps with that of other islet-enriched transcription factors.

Previous reports have suggested that islet enriched transcription factors often bind in close proximity to one another (Ediger et al., 2017). Moreover, immunoprecipitation assays indicated that GLIS3 is associated with PDX1, NEUROD1, and MAFA protein complexes (Yang et al., 2009). Indeed, motif analysis of GLIS3 ChIP-seq identified a number of additional motifs, including motifs for NEUROD1, FOX and RFX family members (FOXM1 and RFX5), and LHX2, which contains a homeobox DNA binding domain similar

to PDX1, NKX6.1, ISL1, and NKX2.2 (Figure 4A). In order to determine whether GLIS3 co-localizes with other islet-enriched transcription factors on the same regulatory regions, we compared GLIS3 binding to that of PDX1, ISL1, NKX6.1, NKX2.2, NEUROD1, MAFA, and FOXA2 (Figure 5A). We also included the ISL1 coactivator LDB1, a critical co-regulator of ISL1 function (Hunter et al., 2013, Ediger et al., 2017). It is important to note that the quality of the ChIP-seq data compared varied greatly, as is typical among various transcription factors. Nevertheless, our analysis revealed that GLIS3 is associated with many of the same promoter/enhancer regions as the transcription factors mentioned above (Figure 5B). In addition to a global analysis, we examined the binding of these factors near the *Ins2*, *Slc2a2*, and *MafA* genes. Figures 5C–E demonstrate the co-localization of GLIS3 binding with that of several other critical islet transcription factors to regulatory regions near the *Ins2*, *Slc2a2*, and *MafA* genes, indicating potential coordination between these transcription factors. Glis3's transcriptional regulation of *MafA* was further supported by luciferase assays of the MafA Region 3 upstream regulatory element. Glis3 stimulated MafA region 3 transcriptional activity, similar to what has been found for other factors (Supplementary Figure 5)(Raum et al., 2006). ChIP-seq binding data showed overlapping binding for almost all of the transcription factors examined, indicating there is likely a high level of coordination between GLIS3 and other islet enriched transcription factors in regulating genes that are critical for normal beta cell function (Figure 5F).

Discussion

Global *Glis3* mutant mice have a short lifespan, develop polycystic kidney disease, hypothyroidism, and exhibit a defect in pancreatic beta cell development that leads to neonatal diabetes (Watanabe et al., 2009, Kang et al., 2009, Yang et al., 2009, Kang et al., 2017). These defects are similar to what is observed in humans with mutations in *GLIS3* (Jetten, 2018). In order to study the function of GLIS3 in the pancreas while limiting secondary effects from other tissues, we developed a conditional mouse model in which GLIS3 function was impaired specifically in the pancreas. Since ubiquitous *Glis3* knockout mice develop hypothyroidism that might influence the pancreatic phenotype (Chen et al., 2018), our model of *Glis3* deletion allows us to examine the role of GLIS3 in beta cell function, while minimizing secondary effects caused by hyperglycemia and hypothyroidism.

Unlike global *Glis3* mutants, which die by PND11 likely due to severe hyperglycemia, $Glis3^{\Delta panc}$ mice begin to develop hyperglycemia around 4-weeks of age dependent upon the efficiency of *Glis3* deletion (Supplementary Figure 1), with almost all $Glis3^{\Delta panc}$ mice surviving until at least 8-weeks of age. As GLIS3 is essential for *Ins2* expression, this indicates that only a subset of functional beta cells (those lacking Cre expression and thus still expressing GLIS3) appear necessary for maintaining euglycemia. Unfortunately, we were unable to test for the persistence of GLIS3 expression due to the lack of a working antibody. However, our interpretation is consistent with a study by Yang et al. showing that in adult mice a ~66% deletion of *Glis3* exon 4, using an tamoxifen-inducible Mouse Insulin Promoter-driven Cre (*MIP-CreERT*), resulted in euglycemic mice, whereas a tamoxifen inducible β-cell specific *Pdx1-CreERT* deletion model with a >90% deletion of *Glis3*, produced hyperglycemic mice (Yang et al., 2017). This conclusion is further supported by a Diptheria toxin-based beta cell ablation model, where a ~50% loss of beta cells does not

cause hyperglycemia, whereas a ~99% ablation does (Thorel et al., 2010). Furthermore, the persistence of some INSULIN$^+$ (Figure 1C) or MAFA$^+$ cells (Figure 2A) is consistent with the mosaicism of the *Pdx1-Cre* that has been observed in other deletion models, such as the Pdx1-Cre deletion of MafA ({Hang, 2014 #55}, where a subset of SLC30A8+ and GLUT2+ cells persist in the islets, likely due to the continued expression of MafA in those cells.

Our analysis of *Glis3*$^{\Delta panc}$ mice revealed no increase in apoptosis at 2-weeks (i.e. prior to hyperglycemia), while proliferation was very slightly increased, possibly in response to an increased demand for insulin$^+$ cells (Figure 2D, F). This stands in contrast to a previous study of GLIS3 function in the thyroid, which demonstrated that GLIS3 does play a role in stimulating proliferation in that tissue (Kang et al., 2017). Moreover, pancreatic ducts in ubiquitous *Glis3* knockout mice, as well as *Glis3*$^{\Delta panc}$ mice (Supplementary Figure 6), did display a cystic phenotype that involves increased proliferation, suggesting that the effect of GLIS3 on proliferation is cell type-dependent. Previous reports suggested that GLIS3 suppresses apoptosis in a pancreatic beta cell line by regulating *Srsf6* (referred to as *Srp55* in (Nogueira et al., 2013)) and in human stem cells differentiated into beta like cells through the TGFβ signaling pathway (Amin et al., 2018). However, in our *in vivo* model, we did not observe an increase in apoptosis, *Srsf6* expression was not changed, nor were apoptotic or TGFβ pathways upregulated in our gene expression analysis (Figure 2F, Supplementary Table 2, and Figure 3A). It is possible that apoptosis is increased at some later time in our model; however, it would be difficult to distinguish this from the secondary effects of hyperglycemia. Instead, we observed changes in genes involved in a variety of metabolic pathways and a downregulation of genes involved in beta cell function (Figure 3A). These results highlight the important, but underappreciated differences that exist between cell line models and *in vivo* mouse systems, which we believe may more accurately reflect the *in vivo* role of GLIS3 in humans.

In addition to a lack of apoptosis, we did not detect expression of the progenitor marker NGN3 in *Glis3*$^{\Delta panc}$ pancreas sections (Supplementary Figure 2), which has been reported to be re-expressed in dedifferentiated β cells (Talchai et al., 2012). This may be expected as GLIS3 is known to function as a positive regulator of *Ngn3* transcription (Kang et al., 2009, Yang et al., 2011, Kim et al., 2012). We also did not observe increased expression of several other dedifferentiation-associated genes, such as *L-myc*, *Oct4*, or *Nanog*, in *Glis3*$^{\Delta panc}$ islets (Supplementary Table 2)(Talchai et al., 2012). These observations suggest that impaired GLIS3 function does not cause dedifferentiation of beta cells; however, we cannot rule out that GLIS3 itself may be required for dedifferentiation. Nevertheless, we did detect a ~12-fold upregulation of *Aldh1a3*, a gene that has been reported to be associated with not only dedifferentiation, but also with beta cell dysfunction (Supplementary Table 2)(Kim-Muller et al., 2016). The expression of *Igfbp4* and *Cxcl12*, “disallowed” genes in pancreatic islets (Pullen et al., 2010, Thorrez et al., 2011), were also upregulated in *Glis3*$^{\Delta panc}$ islets. However, the vast majority of disallowed genes were not induced, including *Ldha*, *Oat*, *Cat*, *Arhgdib*, *Mct1*, *Maf*, *Zfp36l1*, *Itih5*, *Pdgfra*, *Lmo4*, *Zyx*, *Smad3*, *Acot7*, *Cox5a*, *Fam59a*, *Gas6*, *Mgst1*, *Nfib*, *Plec1*, *Rpl36*, *Tgm2*, *Tst*, and *Zdhh*. These findings are consistent with the concept that *Glis3*$^{\Delta panc}$ beta cells do not exhibit a dedifferentiated phenotype, but remain as non-insulin producing, dysfunctional β-like cells.

The coordinated binding of transcription factors at “super” enhancer regions, regions bound by several tissue specific transcription factors for control of tissue specific genes, has been well documented (Loven et al., 2013, Whyte et al., 2013). Within the pancreatic islet, such enhancers have linked not only the binding of islet enriched transcription factors with histone marks of enhancers, but also with mutations related to the development of diabetes and dysregulated fasting glycemia (Pasquali et al., 2014, Stitzel et al., 2010). Analysis of the consensus GLIS3 binding motif suggested co-localization with motifs of other transcription factors important for the regulation of pancreatic β cell functions, such as NEUROD1, FOX and RFX family members, and the homeobox containing Lhx2 (similar to PDX1, NKX6.1, ISL1, and NKX2.2)(Figure 4A). We therefore sought to characterize GLIS3 binding in the context of other islet-enriched transcription factors. Ediger *et al.* recently described the binding of ISL1 in pancreatic islets, where ISL1 largely co-localized with other islet-enriched transcription factors (Ediger et al., 2017). Indeed, we observed that 50% of ISL1 sites overlapped with GLIS3 binding (Figure 5B). In contrast, we observed that GLIS3 only co-localizes with other islet-enriched transcription factors at a fraction of their target sites. A likely explanation for this is the significantly larger number of ChIP-seq peaks called in our GLIS3 analysis, as compared to the ISL1, MAFA, NEUROD1, and FOXA2 ChIP-seq data analysis (Figure 5B). However, even when comparing GLIS3 ChIP-seq data to transcription factors with more peaks (PDX1 and NKX6.1), overlap was limited to <25%. This suggests that islet-enriched transcription factors, including GLIS3, display context-specific co-localization, possibly reflecting tissue specific function. Indeed, genes with nearby overlapping peaks for GLIS3, PDX1, and NKX6.1 were associated particularly with Maturity Onset Diabetes of Young (MODY), insulin resistance, insulin signaling, Type 2 Diabetes, and insulin secretion pathways (Supplementary Figure 7). This supports a model in which a selective set of genes directly regulated by GLIS3 are co-regulated with other islet-enriched transcription factors through their interaction on the same distinct regulatory regions in beta cell-specific genes (Figure 5F). GLIS3 and other islet-specific transcription factors may then coordinate their transcriptional regulation through co-activator protein complexes recruited to these regulatory hubs.

In summary, our study provides the first in depth characterization of the role of GLIS3 in gene regulation within the pancreatic beta cell. GLIS3 has many functions within the beta cell, from regulating aspects of several metabolic pathways and intracellular signaling pathways, to regulating other transcription factors. Indeed, some of the effects on beta cell function could be attributed to GLIS3’s direct regulation of *MafA* through its region 3 regulatory domain (Figure 5E). MAFA has been shown to control expression of *Ins2*, *Slc2a2*, *Slc30a8*, *Sytl4*, and *Stxbp1* all of which are downregulated in $Glis3^{\Delta panc}$ mice (Hang et al., 2014). Unlike $Glis3^{\Delta panc}$ mice, the main defect in $MafA^{\Delta panc}$ mice appears to be in glucose-stimulated insulin secretion, as they do not display overt hyperglycemia. Additionally, GLIS3 regulates a variety of genes not apparently regulated by MAFA, such as *Ngn3* and *Nkx6.1*. GLIS3 is also expressed in variety of tissues which do not express MAFA, indicative of GLIS3’s role in controlling pathways not directly related to beta cell function.

Recent reports have highlighted the importance of phosphorylation in mediating NGN3’s reprogramming effects (Azzarelli et al., 2018), and MAFA’s interaction with other

transcription factors (Han et al., 2016). As GLIS3 is highly phosphorylated, it is likely that GLIS3 transcriptional activity is controlled by upstream and tissue-specific signaling pathways. What these signals are, and how GLIS3 integrates them into co-regulatory interactions or activation/repression functions, remains to be discovered. Understanding how GLIS3 coordinates with other factors, and specifically which upstream signals control GLIS3 activity and guide protein-protein interactions *in vivo*, might provide new therapies for diabetes treatment. Future studies will hopefully build upon the findings outlined here to distinguish how GLIS3 differentially regulates disease-relevant genes in different tissues, which upstream signaling pathways control GLIS3 activity, and provide insight into how these pathways may be targeted in disease treatment.

Supplementary Material

Refer to Web version on PubMed Central for supplementary material.

Acknowledgments:

We would like to thank Molly Cook, Nicole Reeves, and the Epigenomics Core Laboratory at NIEHS for their assistance in high throughput sequencing. We would also like to thank Dr. Chad Hunter at the University of Alabama-Birmingham for assistance in review of this manuscript, and the Cell Biology group at NIEHS for thoughtful comments throughout.

Funding: This research was supported by the Intramural Research Program of the NIEHS, NIH Z01-ES-101585.

References

AMIN S, COOK B, ZHOU T, GHAZIZADEH Z, LIS R, ZHANG T, KHALAJ M, CRESPO M, PERERA M, XIANG JZ, et al. 2018 Discovery of a drug candidate for GLIS3-associated diabetes. Nat Commun, 9, 2681. [PubMed: 29992946]

AZZARELLI R, RULANDS S, NESTOROWA S, DAVIES J, CAMPINOTI S, GILLOTIN S, BONFANTI P, GOTTGENS B, HUCH M, SIMONS B, et al. 2018 Neurogenin3 phosphorylation controls reprogramming efficiency of pancreatic ductal organoids into endocrine cells. Sci Rep, 8, 15374. [PubMed: 30337647]

BARRETT JC, CLAYTON DG, CONCANNON P, AKOLKAR B, COOPER JD, ERLICH HA, JULIER C, MORAHAN G, NERUP J, NIERRAS C, et al. 2009 Genome-wide association study and meta-analysis find that over 40 loci affect risk of type 1 diabetes. Nat Genet, 41, 703–7. [PubMed: 19430480]

BEAK JY, KANG HS, KIM YS & JETTEN AM 2008 Functional analysis of the zinc finger and activation domains of Glis3 and mutant Glis3(NDH1). Nucleic Acids Res, 36, 1690–702. [PubMed: 18263616]

CHEN C, XIE Z, SHEN Y & XIA SF 2018 The Roles of Thyroid and Thyroid Hormone in Pancreas: Physiology and Pathology. Int J Endocrinol, 2018, 2861034. [PubMed: 30013597]

CHO YS, CHEN CH, HU C, LONG J, ONG RT, SIM X, TAKEUCHI F, WU Y, GO MJ, YAMAUCHI T, et al. 2011 Meta-analysis of genome-wide association studies identifies eight new loci for type 2 diabetes in east Asians. Nat Genet, 44, 67–72. [PubMed: 22158537]

DIMITRI P, WARNER JT, MINTON JA, PATCH AM, ELLARD S, HATTERSLEY AT, BARR S, HAWKES D, WALES JK & GREGORY JW 2011 Novel GLIS3 mutations demonstrate an extended multisystem phenotype. Eur J Endocrinol, 164, 437–43. [PubMed: 21139041]

DOBIN A, DAVIS CA, SCHLESINGER F, DRENKOW J, ZALESKI C, JHA S, BATUT P, CHAISSON M & GINGERAS TR 2013 STAR: ultrafast universal RNA-seq aligner. Bioinformatics, 29, 15–21. [PubMed: 23104886]

DUPUIS J, LANGENBERG C, PROKOPENKO I, SAXENA R, SORANZO N, JACKSON AU, WHEELER E, GLAZER NL, BOUATIA-NAJI N, GLOYN AL, et al. 2010 New genetic loci

implicated in fasting glucose homeostasis and their impact on type 2 diabetes risk. Nat Genet, 42, 105–16. [PubMed: 20081858]

EDIGER BN, LIM HW, JULIANA C, GROFF DN, WILLIAMS LT, DOMINGUEZ G, LIU JH, TAYLOR BL, WALP ER, KAMESWARAN V, et al. 2017 LIM domain-binding 1 maintains the terminally differentiated state of pancreatic beta cells. J Clin Invest, 127, 215–229. [PubMed: 27941246]

HABEB AM, AL-MAGAMSI MS, EID IM, ALI MI, HATTERSLEY AT, HUSSAIN K & ELLARD S 2012 Incidence, genetics, and clinical phenotype of permanent neonatal diabetes mellitus in northwest Saudi Arabia. Pediatr Diabetes, 13, 499–505. [PubMed: 22060631]

HAN SI, TSUNEKAGE Y & KATAOKA K 2016 Phosphorylation of MafA enhances interaction with Beta2/NeuroD1. Acta Diabetol, 53, 651–60. [PubMed: 27017486]

HANG Y, YAMAMOTO T, BENNINGER RK, BRISSOVA M, GUO M, BUSH W, PISTON DW, POWERS AC, MAGNUSON M, THURMOND DC, et al. 2014 The MafA transcription factor becomes essential to islet beta-cells soon after birth. Diabetes, 63, 1994–2005. [PubMed: 24520122]

HEINZ S, BENNER C, SPANN N, BERTOLINO E, LIN YC, LASLO P, CHENG JX, MURRE C, SINGH H & GLASS CK 2010 Simple combinations of lineage-determining transcription factors prime cis-regulatory elements required for macrophage and B cell identities. Mol Cell, 38, 576–89. [PubMed: 20513432]

HINGORANI SR, PETRICOIN EF, MAITRA A, RAJAPAKSE V, KING C, JACOBETZ MA, ROSS S, CONRADS TP, VEENSTRA TD, HITT BA, et al. 2003 Preinvasive and invasive ductal pancreatic cancer and its early detection in the mouse. Cancer Cell, 4, 437–50. [PubMed: 14706336]

HU Z & TEE WW 2017 Enhancers and chromatin structures: regulatory hubs in gene expression and diseases. Biosci Rep, 37.

HUANG DA W, SHERMAN BT & LEMPICKI RA 2009a Bioinformatics enrichment tools: paths toward the comprehensive functional analysis of large gene lists. Nucleic Acids Res, 37, 1–13. [PubMed: 19033363]

HUANG DA W, SHERMAN BT & LEMPICKI RA 2009b Systematic and integrative analysis of large gene lists using DAVID bioinformatics resources. Nat Protoc, 4, 44–57. [PubMed: 19131956]

HUNTER CS, DIXIT S, COHEN T, EDIGER B, WILCOX C, FERREIRA M, WESTPHAL H, STEIN R & MAY CL 2013 Islet alpha-, beta-, and delta-cell development is controlled by the Ldb1 coregulator, acting primarily with the islet-1 transcription factor. Diabetes, 62, 875–86. [PubMed: 23193182]

JETTEN AM 2018 GLIS1–3 transcription factors: critical roles in the regulation of multiple physiological processes and diseases. Cell Mol Life Sci, 75, 3473–3494. [PubMed: 29779043]

KANG HS, KIM YS, ZERUTH G, BEAK JY, GERRISH K, KILIC G, SOSA-PINEDA B, JENSEN J, PIERREUX CE, LEMAIGRE FP, et al. 2009 Transcription factor Glis3, a novel critical player in the regulation of pancreatic beta-cell development and insulin gene expression. Mol Cell Biol, 29, 6366–79. [PubMed: 19805515]

KANG HS, KUMAR D, LIAO G, LICHTI-KAISER K, GERRISH K, LIAO XH, REFETOFF S, JOTHI R & JETTEN AM 2017 GLIS3 is indispensable for TSH/TSHR-dependent thyroid hormone biosynthesis and follicular cell proliferation. J Clin Invest, 127, 4326–4337. [PubMed: 29083325]

KANG HS, TAKEDA Y, JEON K & JETTEN AM 2016 The Spatiotemporal Pattern of Glis3 Expression Indicates a Regulatory Function in Bipotent and Endocrine Progenitors during Early Pancreatic Development and in Beta, PP and Ductal Cells. PLoS One, 11, e0157138. [PubMed: 27270601]

KANG HS, ZERUTH G, LICHTI-KAISER K, VASANTH S, YIN Z, KIM YS & JETTEN AM 2010 Gli-similar (Glis) Kruppel-like zinc finger proteins: insights into their physiological functions and critical roles in neonatal diabetes and cystic renal disease. Histol Histopathol, 25, 1481–96. [PubMed: 20865670]

KIM-MULLER JY, FAN J, KIM YJ, LEE SA, ISHIDA E, BLANER WS & ACCILI D 2016 Aldehyde dehydrogenase 1a3 defines a subset of failing pancreatic beta cells in diabetic mice. Nat Commun, 7, 12631. [PubMed: 27572106]

KIM YS, KANG HS, TAKEDA Y, HOM L, SONG HY, JENSEN J & JETTEN AM 2012 Glis3 regulates neurogenin 3 expression in pancreatic beta-cells and interacts with its activator, Hnf6. Mol Cells, 34, 193–200. [PubMed: 22820919]

LANGMEAD B, TRAPNELL C, POP M & SALZBERG SL 2009 Ultrafast and memory-efficient alignment of short DNA sequences to the human genome. Genome Biol, 10, R25. [PubMed: 19261174]

LIAO Y, SMYTH GK & SHI W 2014 featureCounts: an efficient general purpose program for assigning sequence reads to genomic features. Bioinformatics, 30, 923–30. [PubMed: 24227677]

LICHTI-KAISER K, ZERUTH G, KANG HS, VASANTH S & JETTEN AM 2012 Gli-similar proteins: their mechanisms of action, physiological functions, and roles in disease. Vitam Horm, 88, 141–71. [PubMed: 22391303]

LIU C, LI H, QI L, LOOS RJ, QI Q, LU L, GAN W & LIN X 2011 Variants in GLIS3 and CRY2 are associated with type 2 diabetes and impaired fasting glucose in Chinese Hans. PLoS One, 6, e21464. [PubMed: 21747906]

LOVE MI, HUBER W & ANDERS S 2014 Moderated estimation of fold change and dispersion for RNA-seq data with DESeq2. Genome Biol, 15, 550. [PubMed: 25516281]

LOVEN J, HOKE HA, LIN CY, LAU A, ORLANDO DA, VAKOC CR, BRADNER JE, LEE TI & YOUNG RA 2013 Selective inhibition of tumor oncogenes by disruption of super-enhancers. Cell, 153, 320–34. [PubMed: 23582323]

LUO W, PANT G, BHAVNASI YK, BLANCHARD SG JR. & BROUWER C 2017 Pathview Web: user friendly pathway visualization and data integration. Nucleic Acids Res, 45, W501–W508. [PubMed: 28482075]

MARTIN M 2011 Cutadapt removes adapater sequences from high throughput sequencing reads. EMBnet journal, 17, 10–12.

NOGUEIRA TC, PAULA FM, VILLATE O, COLLI ML, MOURA RF, CUNHA DA, MARSELLI L, MARCHETTI P, CNOP M, JULIER C, et al. 2013 GLIS3, a susceptibility gene for type 1 and type 2 diabetes, modulates pancreatic beta cell apoptosis via regulation of a splice variant of the BH3-only protein Bim. PLoS Genet, 9, e1003532. [PubMed: 23737756]

PASQUALI L, GAULTON KJ, RODRIGUEZ-SEGUI SA, MULARONI L, MIGUEL-ESCALADA I, AKERMAN I, TENA JJ, MORAN I, GOMEZ-MARIN C, VAN DE BUNT M, et al. 2014 Pancreatic islet enhancer clusters enriched in type 2 diabetes risk-associated variants. Nat Genet, 46, 136–143. [PubMed: 24413736]

PULLEN TJ, KHAN AM, BARTON G, BUTCHER SA, SUN G & RUTTER GA 2010 Identification of genes selectively disallowed in the pancreatic islet. Islets, 2, 89–95. [PubMed: 21099300]

QUINLAN AR & HALL IM 2010 BEDTools: a flexible suite of utilities for comparing genomic features. Bioinformatics, 26, 841–2. [PubMed: 20110278]

RAUM JC, GERRISH K, ARTNER I, HENDERSON E, GUO M, SUSSEL L, SCHISLER JC, NEWGARD CB & STEIN R 2006 FoxA2, Nkx2.2, and PDX-1 regulate islet beta-cell-specific mafA expression through conserved sequences located between base pairs −8118 and −7750 upstream from the transcription start site. Mol Cell Biol, 26, 5735–43. [PubMed: 16847327]

REES SD, HYDRIE MZ, O'HARE JP, KUMAR S, SHERA AS, BASIT A, BARNETT AH & KELLY MA 2011 Effects of 16 genetic variants on fasting glucose and type 2 diabetes in South Asians: ADCY5 and GLIS3 variants may predispose to type 2 diabetes. PLoS One, 6, e24710. [PubMed: 21949744]

SCOVILLE DW, KANG HS & JETTEN AM 2017 GLIS1–3: emerging roles in reprogramming, stem and progenitor cell differentiation and maintenance. Stem Cell Investig, 4, 80.

SENEE V, CHELALA C, DUCHATELET S, FENG D, BLANC H, COSSEC JC, CHARON C, NICOLINO M, BOILEAU P, CAVENER DR, et al. 2006 Mutations in GLIS3 are responsible for a rare syndrome with neonatal diabetes mellitus and congenital hypothyroidism. Nat Genet, 38, 682–7. [PubMed: 16715098]

STITZEL ML, SETHUPATHY P, PEARSON DS, CHINES PS, SONG L, ERDOS MR, WELCH R, PARKER SC, BOYLE AP, SCOTT LJ, et al. 2010 Global epigenomic analysis of primary human pancreatic islets provides insights into type 2 diabetes susceptibility loci. Cell Metab, 12, 443–55. [PubMed: 21035756]

TALCHAI C, XUAN S, LIN HV, SUSSEL L & ACCILI D 2012 Pancreatic beta cell dedifferentiation as a mechanism of diabetic beta cell failure. Cell, 150, 1223–34. [PubMed: 22980982]

THOREL F, NEPOTE V, AVRIL I, KOHNO K, DESGRAZ R, CHERA S & HERRERA PL 2010 Conversion of adult pancreatic alpha-cells to beta-cells after extreme beta-cell loss. Nature, 464, 1149–54. [PubMed: 20364121]

THORREZ L, LAUDADIO I, VAN DEUN K, QUINTENS R, HENDRICKX N, GRANVIK M, LEMAIRE K, SCHRAENEN A, VAN LOMMEL L, LEHNERT S, et al. 2011 Tissue-specific disallowance of housekeeping genes: the other face of cell differentiation. Genome Res, 21, 95–105. [PubMed: 21088282]

WATANABE N, HIRAMATSU K, MIYAMOTO R, YASUDA K, SUZUKI N, OSHIMA N, KIYONARI H, SHIBA D, NISHIO S, MOCHIZUKI T, et al. 2009 A murine model of neonatal diabetes mellitus in Glis3-deficient mice. FEBS Lett, 583, 2108–13. [PubMed: 19481545]

WEN X & YANG Y 2017 Emerging roles of GLIS3 in neonatal diabetes, type 1 and type 2 diabetes. J Mol Endocrinol, 58, R73–R85. [PubMed: 27899417]

WHYTE WA, ORLANDO DA, HNISZ D, ABRAHAM BJ, LIN CY, KAGEY MH, RAHL PB, LEE TI & YOUNG RA 2013 Master transcription factors and mediator establish super-enhancers at key cell identity genes. Cell, 153, 307–19. [PubMed: 23582322]

YANG Y, BUSH SP, WEN X, CAO W & CHAN L 2017 Differential Gene Dosage Effects of Diabetes-Associated Gene GLIS3 in Pancreatic beta Cell Differentiation and Function. Endocrinology, 158, 9–20. [PubMed: 27813676]

YANG Y, CHANG BH & CHAN L 2013 Sustained expression of the transcription factor GLIS3 is required for normal beta cell function in adults. EMBO Mol Med, 5, 92–104. [PubMed: 23197416]

YANG Y, CHANG BH, SAMSON SL, LI MV & CHAN L 2009 The Kruppel-like zinc finger protein Glis3 directly and indirectly activates insulin gene transcription. Nucleic Acids Res, 37, 2529–38. [PubMed: 19264802]

YANG Y, CHANG BH, YECHOOR V, CHEN W, LI L, TSAI MJ & CHAN L 2011 The Kruppel-like zinc finger protein GLIS3 transactivates neurogenin 3 for proper fetal pancreatic islet differentiation in mice. Diabetologia, 54, 2595–605. [PubMed: 21786021]

ZERUTH GT, TAKEDA Y & JETTEN AM 2013 The Kruppel-like protein Gli-similar 3 (Glis3) functions as a key regulator of insulin transcription. Mol Endocrinol, 27, 1692–705. [PubMed: 23927931]

ZHOU Q, LAW AC, RAJAGOPAL J, ANDERSON WJ, GRAY PA & MELTON DA 2007 A multipotent progenitor domain guides pancreatic organogenesis. Dev Cell, 13, 103–14. [PubMed: 17609113]

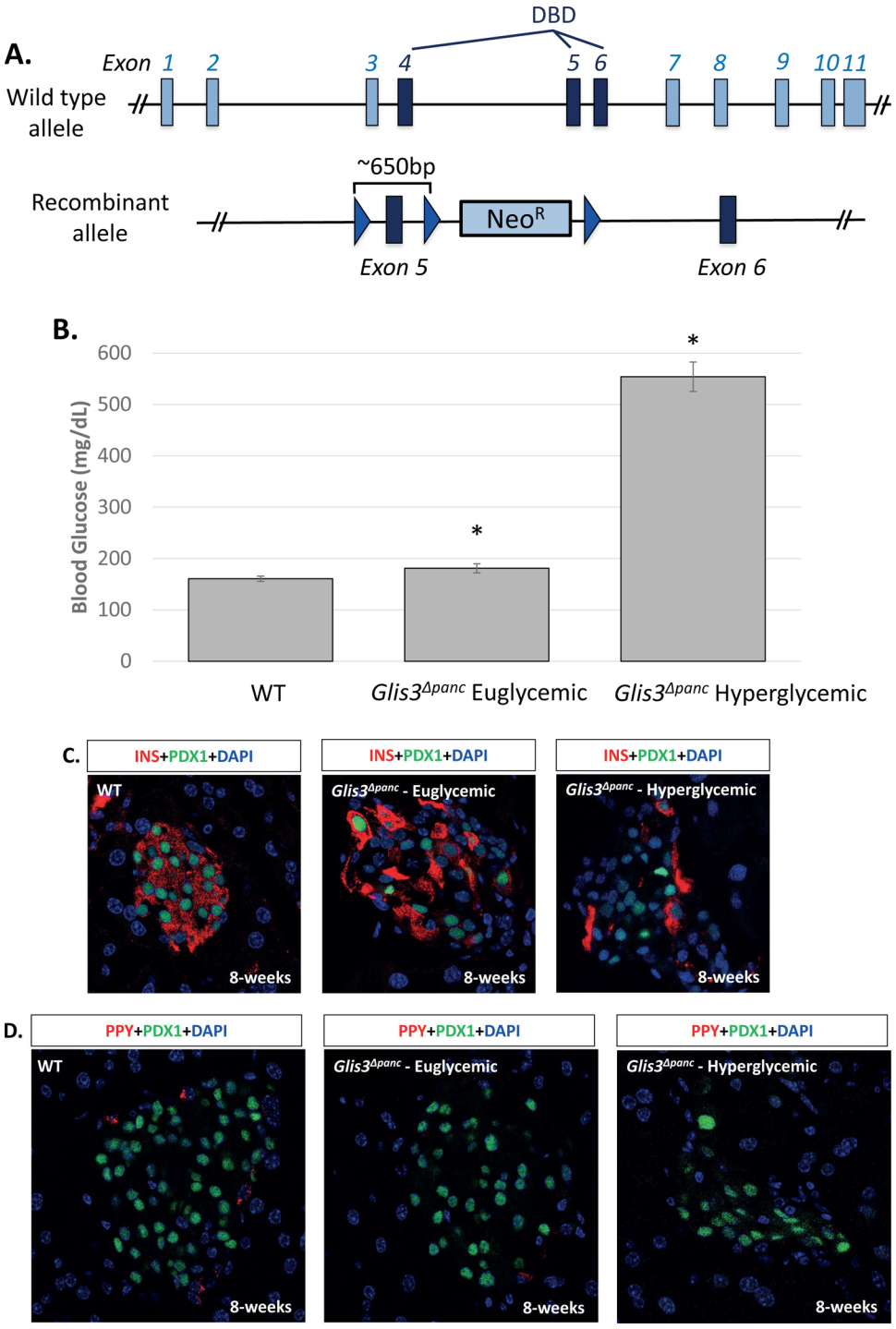

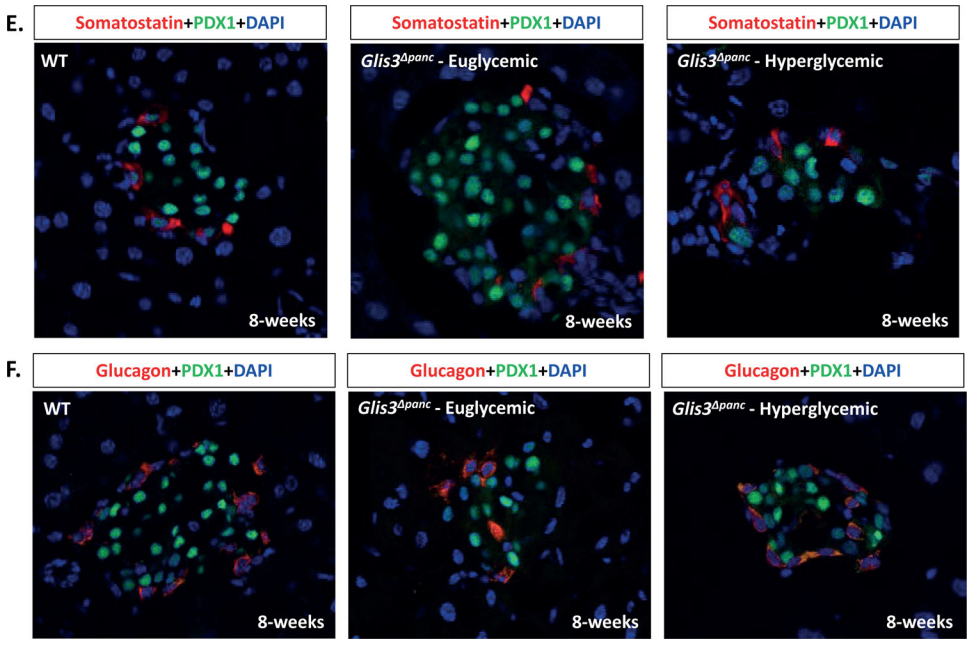

Figure 1. *Glis3*$^{\Delta panc}$ mice exhibit a loss of insulin-producing beta cells.

(A) Schematic of wild type and recombinant *Glis3* allele. A conditional knockout allele for the *Glis3* gene was generated in C57BL/6 mice containing loxP sites (triangles) surrounding exon 5 of *Glis3*. Exons 4–6 encode the DNA-binding domain (DBD). Mice were bred with a strain expressing Cre recombinase under the control of the *Pdx1* promoter. **(B)** Random blood glucose levels of mice at 8-weeks of age. *Glis3*$^{\Delta panc}$ mice were grouped as either Euglycemic (<250 mg/dL) or Hyperglycemic (>250 mg/dL) and compared to control littermates (WT) (N=11 WT, N=5 *Glis3*$^{\Delta panc}$ euglycemic, N=4 *Glis3*$^{\Delta panc}$ hyperglycemic). Immunofluorescence staining revealed a reduction in the number of INS^{+}PDX1^{+} beta cells **(C)** and pancreatic polypeptide^{+} cells **(D)**, with no apparent effect on **(E)** glucagon or **(F)** somatostatin expression. Nuclei were visualized by DAPI staining. Representative images are shown. * indicates $p<0.05$.

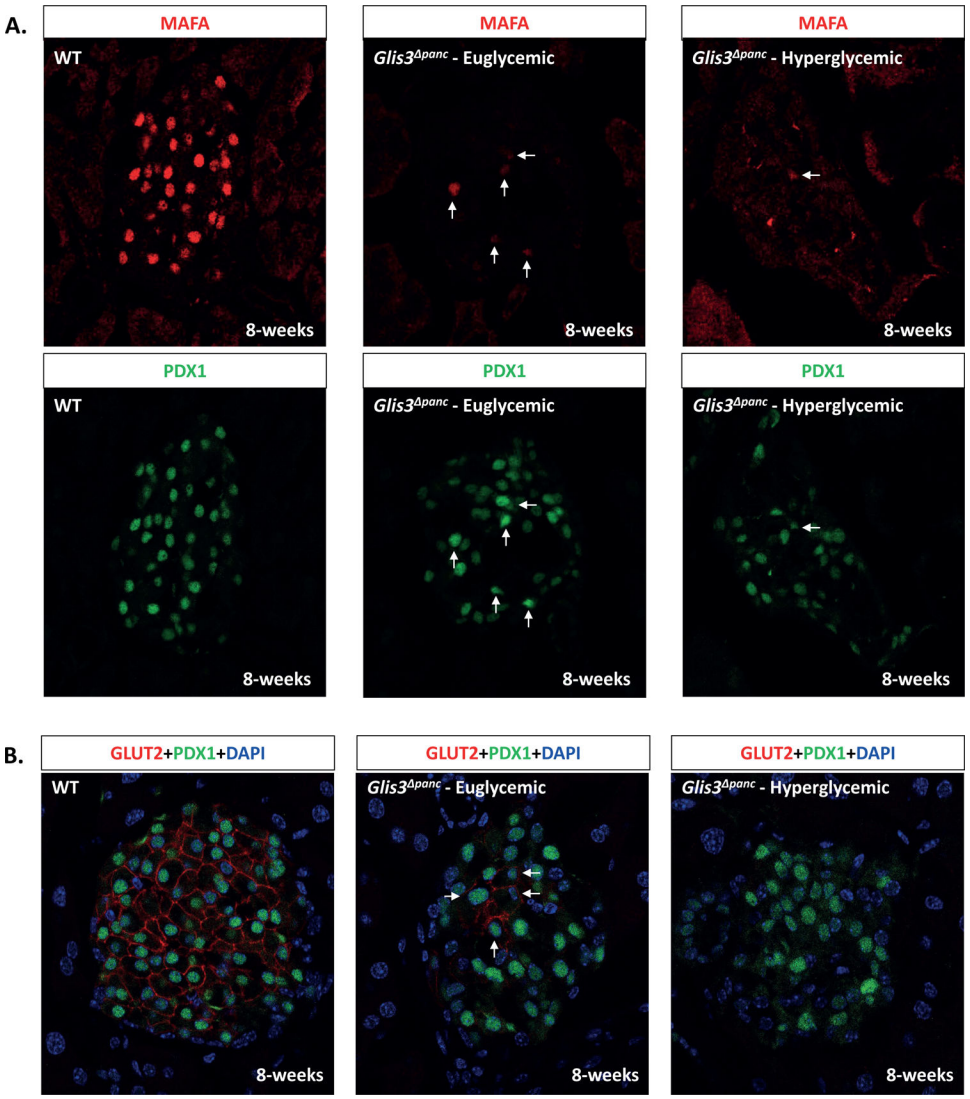

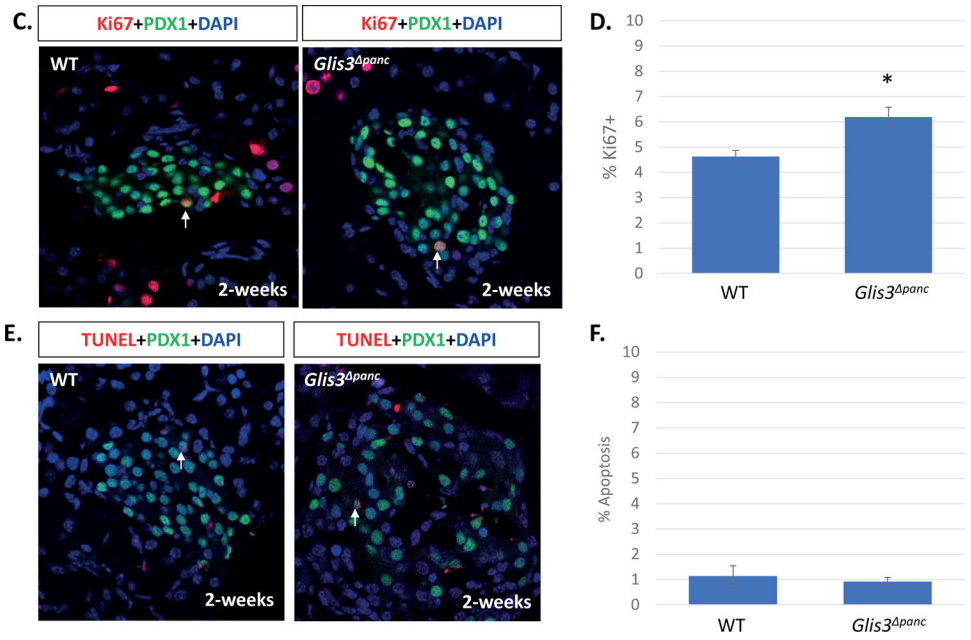

Figure 2. Beta cells lose key markers, but do not apoptose in *Glis3*$^{\Delta panc}$ mice.

Pancreas sections from 8-week-old *Glis3*$^{\Delta panc}$ mice were stained for PDX1 and MAFA **(A)** or GLUT2 **(B)**. Proliferation was measured via Ki67 and PDX1 double staining of 2-week old *Glis3*$^{\Delta panc}$ mice **(C)**, and quantified **(D)**. Apoptosis was measured via TUNEL and PDX1 double staining of 2-week old *Glis3*$^{\Delta panc}$ mice **(E)**, and quantified **(F)**. Results from N=3 mice for each genotype, error bars = SEM, * indicates $p<0.05$. Arrows indicate MAFA $^{+}$PDX1^{+} (A), GLUT2^{+}PDX1^{+} (B), Ki67^{+}PDX1^{+} (C), or TUNEL^{+}PDX1^{+} (D) cells. Representative images are shown.

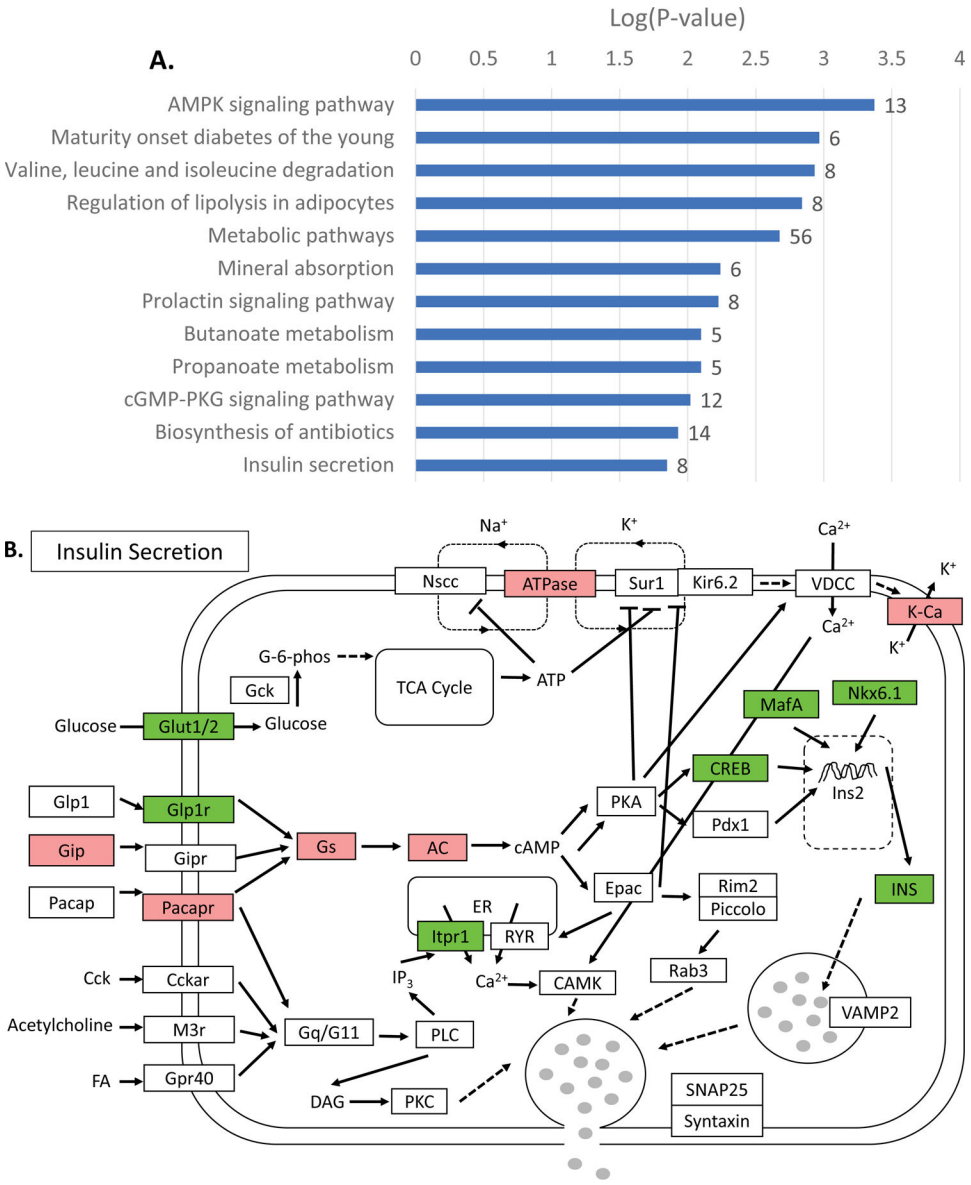

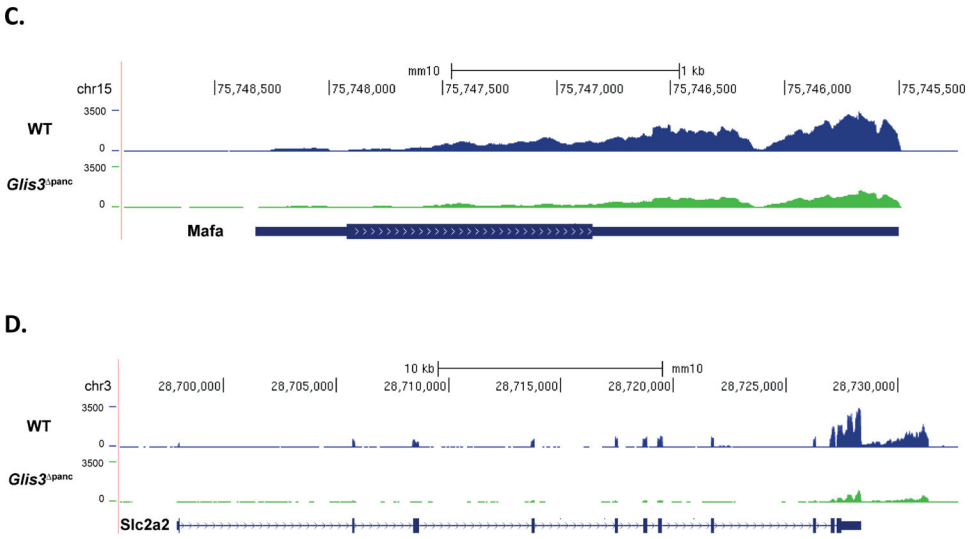

Figure 3. Gene expression analysis of *Glis3*$^{\Delta panc}$ mice.

RNA-seq analysis of *Glis3*$^{\Delta panc}$ islets at 4-weeks was performed. **(A)** KEGG pathway analysis of genes downregulated >1.5 fold and with an FDR of <0.05. Numbers behind bars indicate number of genes in the respective pathway. **(B)** Modified Pathview analysis of the Insulin Secretion pathway genes, with green representing downregulated genes and red representing upregulated genes. RNA-seq analysis of **(C)** *MafA* and **(D)** *Slc2a2*, the gene that encodes the GLUT2 protein. Data displayed via the UCSC genome browser. N=3 *Glis3*$^{\Delta panc}$, N=4 WT.

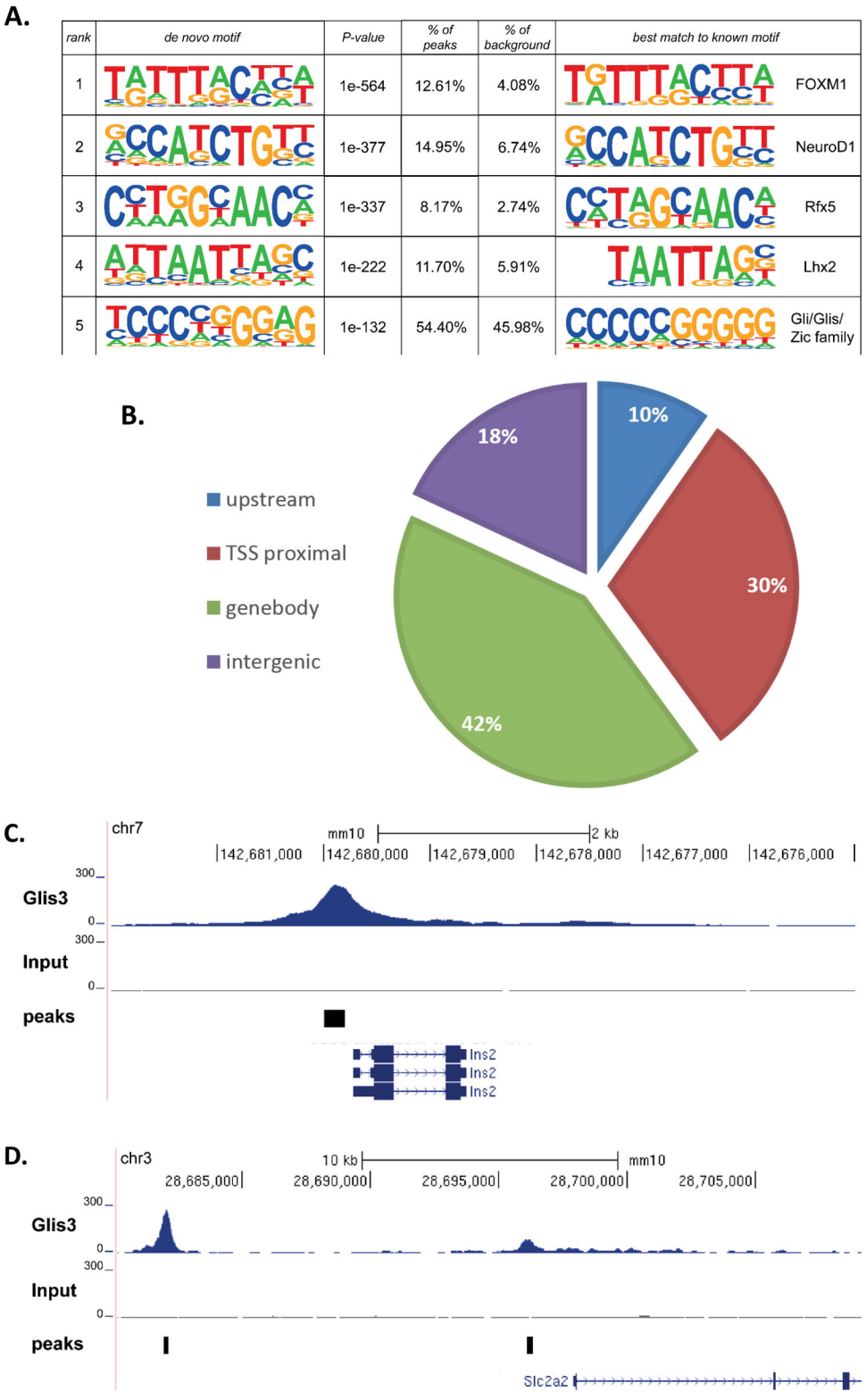

Figure 4. Global GLIS3 binding analysis in mouse islets reveals *Slc2a2* direct regulation.

(A) *De novo* motif analysis was performed on ChIP-seq data using HOMER. **(B)** Binding analysis of Glis3 ChIP-seq data indicated a preference for introns and promoters. Upstream

= −10kb to −1kb relative to TSS, TSS proximal = −1kb to TSS, Gene body = TSS to TES, Intergenic = remaining sequences. **(C,D)** ChIP-seq binding on the *Ins2* promoter, and the *Slc2a2* promoter and enhancer. Peaks indicates the peaks called using HOMER.

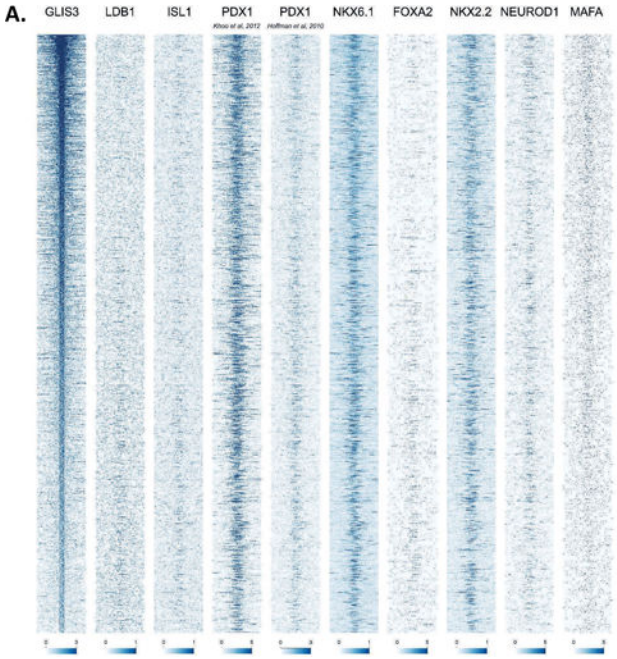

B.

ChIP	peaks	% Glis3 peaks/ TF peaks
GLIS3	21,254	100.0%
LDB1	1,842	38%
ISL1	1,147	50%
PDX1 (Khoo et al. 2012)	50,072	22%
PDX1 (Hoffman et al 2010)	6,945	34%
NKX6.1	34,711	14%
FOXA2	4,225	30%
NKX2.2	12,186	25%
NEUROD1	4,769	48%
MAFA	1,173	41%

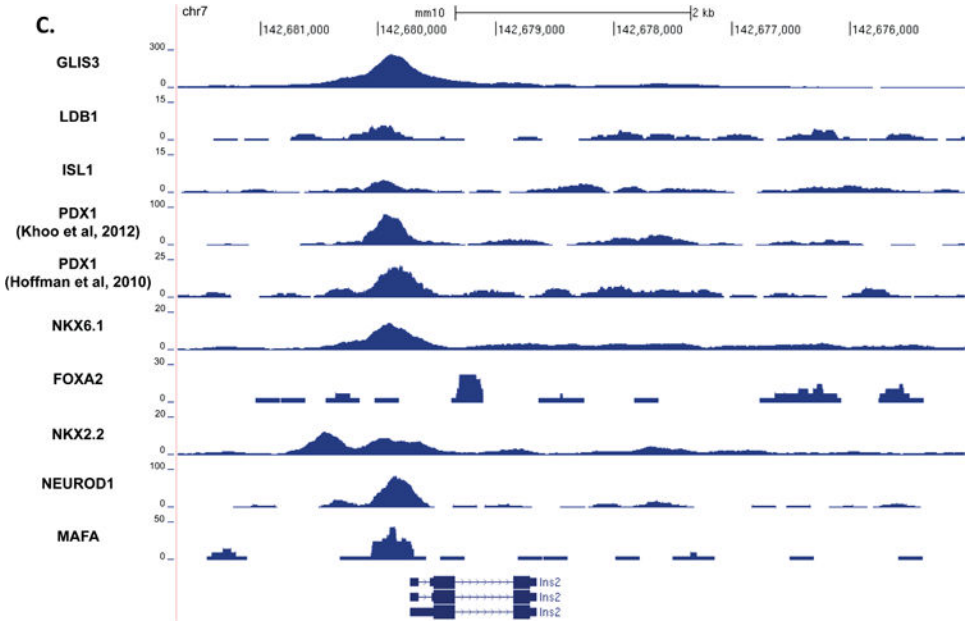

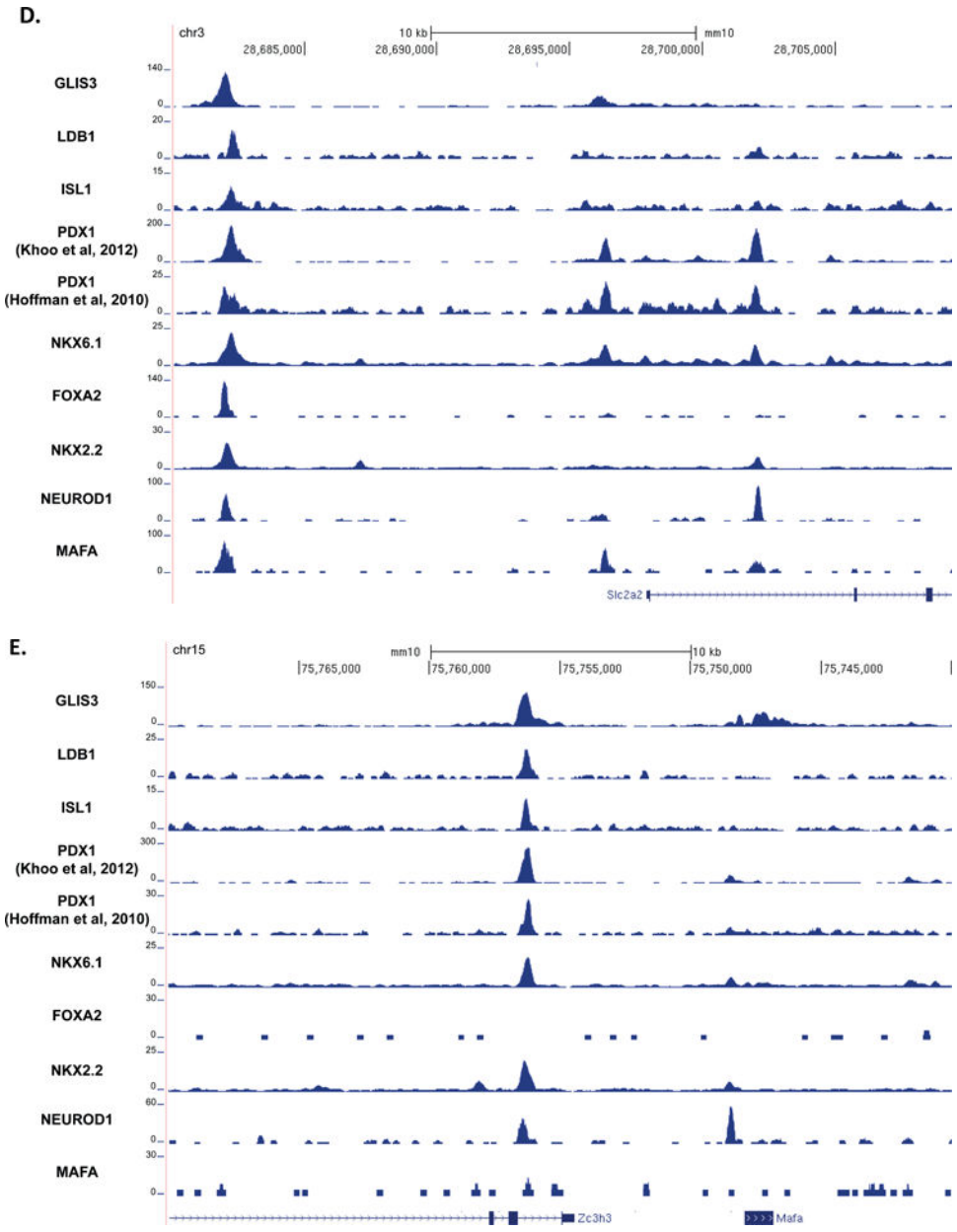

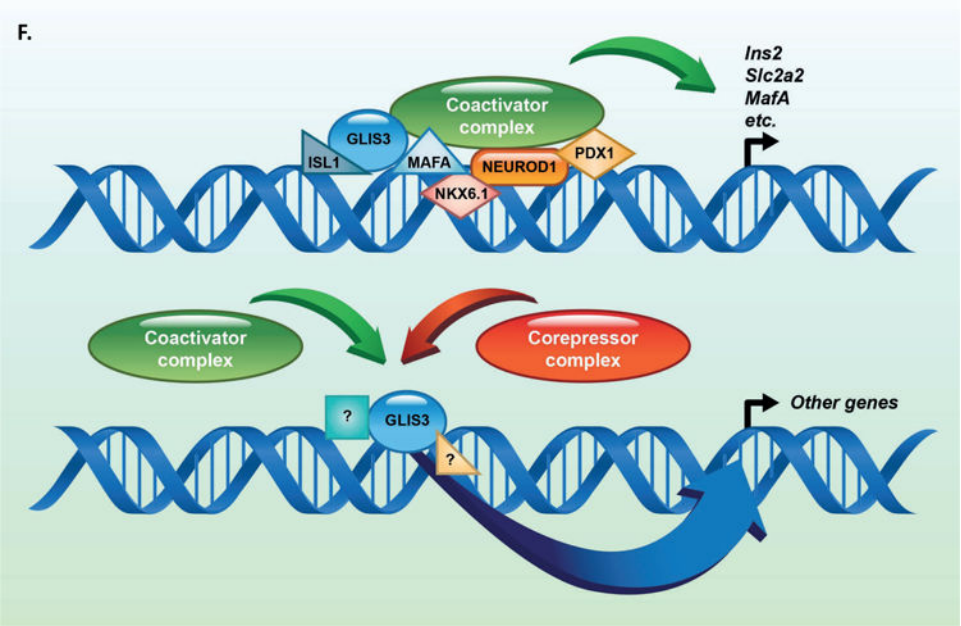

Figure 5. GLIS3 binding shows partial overlap with other islet enriched transcription factors.

(A) Heatmap of the 2kb region centered on each of the 21,253 GLIS3 binding peaks with ChIP-seq signal normalized to 10 million reads for GLIS3, LDB1, ISL1, PDX1 (from two independent labs), NKX6.1, FOXA2, NKX2.2, NEUROD1, and MAFA. Color intensity indicates read depth, as shown by the scale below each TF panel. **(B)** Number of peaks called for each ChIP, as well as percentage of TF ChIP peaks colocalizing with GLIS3 peaks with signal above threshold cutoff. ChIP peak colocalization near the *Ins2* **(C)**, *Slc2a2* **(D)**, and *MafA* **(E)** genes. Data displayed via the UCSC genome browser. **(F)** Model of GLIS3 binding. Glis3 interacts with islet enriched transcription factors on regulatory hubs to control genes related to diabetes, and interacts with other unknown factors to recruit either coactivator or corepressor complexes to control genes related to other processes.

Table 1.

Islet-specific genes are bound by GLIS3

Hormones			
Gene	**Fold Change**	**FDR**	**Glis3 ChIP-seq Signal**
Ins1	−2.116517315	0.00506878	yes
Ins2	−2.839350013	3.35E-13	yes
Ppy	−8.154862239	1.87E-19	yes
Gcg	−1.234894439	NS	no
Sst	1.083293292	NS	no
Ghrl	1.095231496	NS	no
Beta cell Function			
Slc2a2	−5.112554821	9.58E-33	yes
Kcnj11	−1.299797953	0.01104388	yes
Abcc8	1.444296553	0.00016462	yes
Glp1r	−1.848329213	0.02182045	yes
Chga	−2.13350168	3.53E-22	yes
Ucn3	−1.588987707	NS	yes
Gjd2	−1.120393715	NS	yes
Transcription Factors			
MafA	−2.693922579	0.00026979	yes
Nkx6.1	−2.239512577	1.03E-09	yes
Rfx6	1.349799675	0.00446909	yes
Isl1	1.640589346	4.17E-10	yes
Ldb1	−1.279981837	0.00500245	yes
MafB	−1.496356376	0.00324023	yes
FoxA2	−1.281876971	0.045365	yes
Pdx1	−1.061699976	NS	yes
Tshz1	1.084110443	NS	yes
Mnx1	1.114782737	NS	yes
InsM1	1.102778676	NS	yes
Ngn3	−1.731654424	NS	yes
Nkx2.2	−1.211137492	NS	yes